Yao *et al. BMC Plant Biology* (2025) 25:1006
https://doi.org/10.1186/s12870-025-07079-4

BMC Plant Biology

RESEARCH Open Access

Combined metabolome and transcriptome to analyze the regulatory network of key enzymes in the synthesis of senkirkine in *Emilia sonchifolia*

Jinli Yao[1,2*], Yanqing Qin[1], Dongping Tu[1*], Yumei Huang[1], Liuguan Liang[1], Wenhui Cai[1], Mingli Huang[1], Xiaoqi Zhu[1] and Xinling Lao[1]

Abstract

Emilia sonchifolia (L.) DC. serves as a well-known folk medicinal and edible plant, yet its toxic component senkirkine exhibits hepatotoxicity. Acute high-dose exposure can induce sinusoidal obstruction syndrome, while chronic low-dose intake may cause hepatic megaloblastosis and fibrosis. This study applied metabolomics to analyze alkaloid compositions in the plant's roots, stems, leaves, and flowers. A total of 91 differential metabolites were detected, belonging to 10 alkaloids, among which pyrrolizidine alkaloids accounted for 13%. Senkirkine showed the most significant content variation between roots and flowers, with roots containing notably higher levels. Transcriptomic analysis identified 119,886 unigenes and 32,797 DEGs. Among these, authors selected 45 key enzymes involved in senkirkine biosynthesis, categorizing them into 7 groups corresponding to 172 candidate enzyme genes. Methyltransferase, alcohol dehydrogenase, acyltransferase, and cyclooxygenase genes expressed more highly in roots than in flowers, matching metabolomic expression patterns. Through qRT-PCR of five key enzyme genes, researchers found that four genes (*BAHD-Ats*, *CCoAOMT*, *BOMT*, *3AT*) peaked in roots, while *CAD* showed highest expression in stems—findings consistent with transcriptomic results. This study provided references for gene functional expression analysis and laid a foundation for decoding the senkirkine biosynthesis pathway. It aims to regulate key enzyme genes to develop low-toxic *E. sonchifolia* resources, integrating metabolomic and transcriptomic approaches to balance medicinal efficacy and safety.

Keywords *Emilia sonchifolia*, Senkirkine, Metabolome, Transcriptome, QRT-PCR

*Correspondence:
Jinli Yao
3448495183@qq.com
Dongping Tu
fairytdp@163.com
[1]Guangxi University of Chinese Medicine, Nanning 530200, China
[2]College of Chemistry and Chemical Engineering, Central South University, Changsha 410000, China

Introduction

Emilia sonchifolia (L.) DC. (*E. sonchifolia*), known as "Yi Dian Hong" or "Zi Bei Cao" in Chinese, belongs to tribe Emilia in the family Asteraceae [1]. It is an annual herb, widely distributed in Guangxi, Yunnan and other places. Its whole plant has the efficacy of clearing heat and detoxifying, anti-inflammatory and diuretic, dispersing blood stasis and reducing swelling so on, and it is commonly used in traditional Chinese medicine and ethnomedicine for treating upper respiratory tract infection, mouth ulcers, urinary tract infections, pneumonia, mastitis, enteritis, traumatic infections etc. in China [2–4]. It is often used to treat inflammation and mosquito bites in India and is commonly used to treat mosquito bites in Brazil [5, 6].

E. sonchifolia is a highly valuable medicinal plant, commonly used as a single herb or as a prescription preparation for a wide range of applications. Among the recorded prescription preparations and single-flavor remedies in the 2015 edition of the Chinese Pharmacopoeia [7], *E. sonchifolia* as the main raw material of the Chinese patent medicine preparation of huahong tablets, the main treatment for menstrual disorders, dysmenorrhoea, endometritis, adnexitis, pelvic inflammation and other gynecological inflammatory diseases [8]. *E. sonchifolia* is a famous edible and medicinal wild vegetable, which contains a variety of nutrients, and it is unique in flavor, fragrant and refreshing. In recent years, *E. sonchifolia* has been developed into a famous wild vegetable that has been put on the table, which is favored by people and has broad application prospects [9].

It was found that the main chemical constituents of *E. sonchifolia* are flavonoids, alkaloids, phenols, and so on [10, 11]. The main alkaloids known to be contained in *E. sonchifolia* to date are senkirkine (Sek), Senecionine N-oxide (SnNO), etc [12]., all of which are pyrrolizidine alkaloids (PAs). At present, scholars at home and abroad have carried out relevant research on the PAs components in *E. sonchifolia*. For example, Ni et al. [13] used ethanol reflux extraction to obtain alkaloid extracts, which were identified as Sek; Cheng et al. [14] isolated and identified PAs polyesterine from *E. sonchifolia*; Shen [15] isolated a little red alkali from *E. sonchifolia*; Ning et al. [1] used HPLC to determine the average content of Sek in the different origins of *E. sonchifolia* was 0.40 $mg{\cdot}g^{-1}$; Zhou et al. [16] analyzed the total alkaloid content of *E. sonchifolia* from different harvesting periods in Guangxi ranged from 4.31 to 13.99 $mg{\cdot}g^{-1}$; Hsieh et al. [17] used GC-MS to identify 11 PAs such as Sek, Seneciphylline (Sp), etc. from *E. sonchifolia*; Luo et al. [18, 19] used UPLC-Q-TOF-MS technology to identify 7 kinds of PAs including Sp from *E. sonchifolia*, and found that *E. sonchifolia* had antioxidant and anti-inflammatory effects.

Studies have found that PAs pose hepatotoxic risks [20, 21]: acute high-dose exposure can cause sinusoidal obstruction syndrome, while chronic low-dose intake may lead to hepatic megaloblastosis and fibrosis [22–27]. The World Health Organization recommends an intake limit of PAs of 0.015 mg kg^{-1} [28]. Given Sek's high content in *E. sonchifolia*, analyzing its toxic components for safe use is an urgent industry priority.

In recent years, with the advancement of multi-omics technologies, metabolome and transcriptome sequencing have been widely applied to study the molecular mechanisms of secondary metabolite biosynthesis in traditional Chinese medicine. You et al. [29] constructed the gene knockout vector of the effector g12593 of Fusarium oxysporum f. sp. cubense by genome-wide and transcriptome techniques, laying a foundation for the prevention and treatment of banana Fusarium wilt; Xu et al. [30] used bioinformatics analysis, transcriptome and other techniques to knock out the up-regulated chitin deacetylase gene in wheat, revealing the molecular mechanism of Fusarium graminearum chitin deacetylase family pathogenesis; Zhang et al. [31] used transcriptomics to knock out 3 protein kinases in the BdGpmk1-MAPK signaling pathway of Botryosphaeria dothidea, which provided a theoretical basis for exploring the molecular mechanism of regulating the growth and development and pathogenicity of Botryosphaeria dothidea.

In this experiment, we analyzed and screened candidate sequences of key enzyme genes in the Sek biosynthetic pathway using metabolome and transcriptome sequencing data of *E. sonchifolia*. These findings were further validated by quantitative real-time PCR (qRT-PCR). The results lay a foundation for future research, including elucidating the Sek and PAs synthesis pathways, regulating key enzyme genes, and breeding *E. sonchifolia* varieties with reduced toxicity. Ultimately, these efforts aim to promote the sustainable development of the *E. sonchifolia* industry.

Results

Metabolomic analysis of alkaloids with *E. sonchifolia*

The total ion current (TIC) plots of different quality control (QC) samples, detected by mass spectrometry, were analyzed through overlapping display. According to the TIC plots (Fig. 1a, b), the curves of different QC samples exhibit high overall overlap, stable signal intensity, and minimal systematic error, confirming the reliability of the detected data for subsequent analysis. Principal Component Analysis (PCA) results demonstrate distinct intra-group clustering for roots, stems, leaves, and flowers samples of *E. sonchifolia*, indicating low within-group variability (Fig. 1c). In the first principal component, stems and leaves show closer similarity to QC samples, whereas roots and flowers display a significant

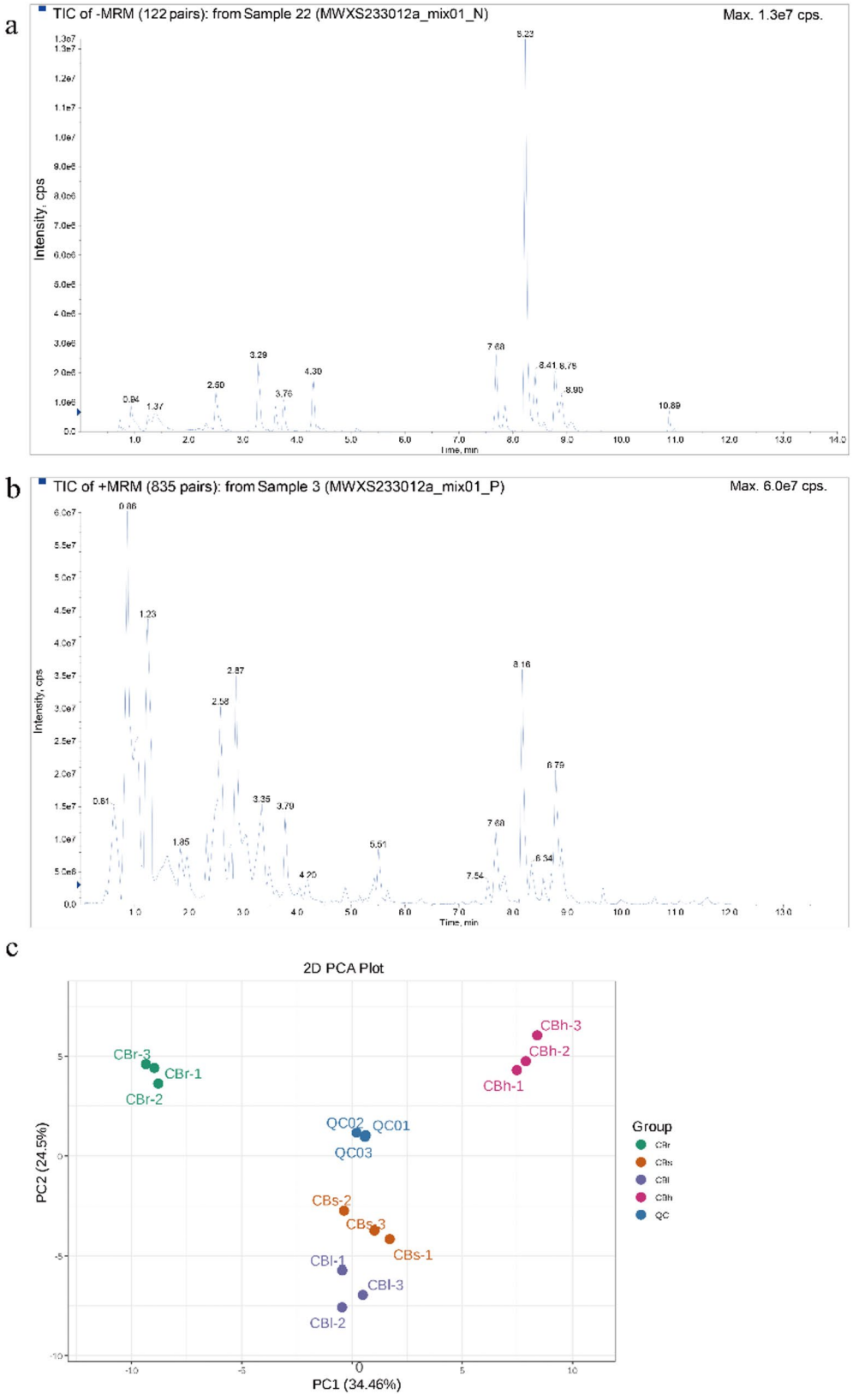

Fig. 1 Qualitative and quantitative analysis of metabolome of *E. sonchifolia*. **a** Sample mass spectrometry detection TIC overlap map-N of *E. sonchifolia*. **b** Sample mass spectrometry detection TIC overlap map-P of *E. sonchifolia*. **c** PCA plot of metabolites in different tissues of *E. sonchifolia*. "CBr" is the sample of roots, "CBs" is the sample of stems, "CBl" is the sample of leaves, "CBh" is the sample of flowers

separation trend, suggesting substantial metabolic differences between roots and flowers in this component. Conversely, in the second principal component, roots and flowers resemble QC samples, while stems and leaves exhibit clear separation, indicating notable metabolic discrepancies in stems and leaves versus minor differences between roots and flowers. According to the orthogonal partial least squares-discriminant analyses (OPLS-DA) score plot, there was a clear trend of separation between the comparison groups of different tissues of *E. sonchifolia* in the horizontal coordinate, while the samples were more aggregated within each group in the vertical coordinate, which indicated that there were inter-group differences between the samples of different tissues of *E. sonchifolia*, while the intra-group reproducibility was higher (Fig. 2).

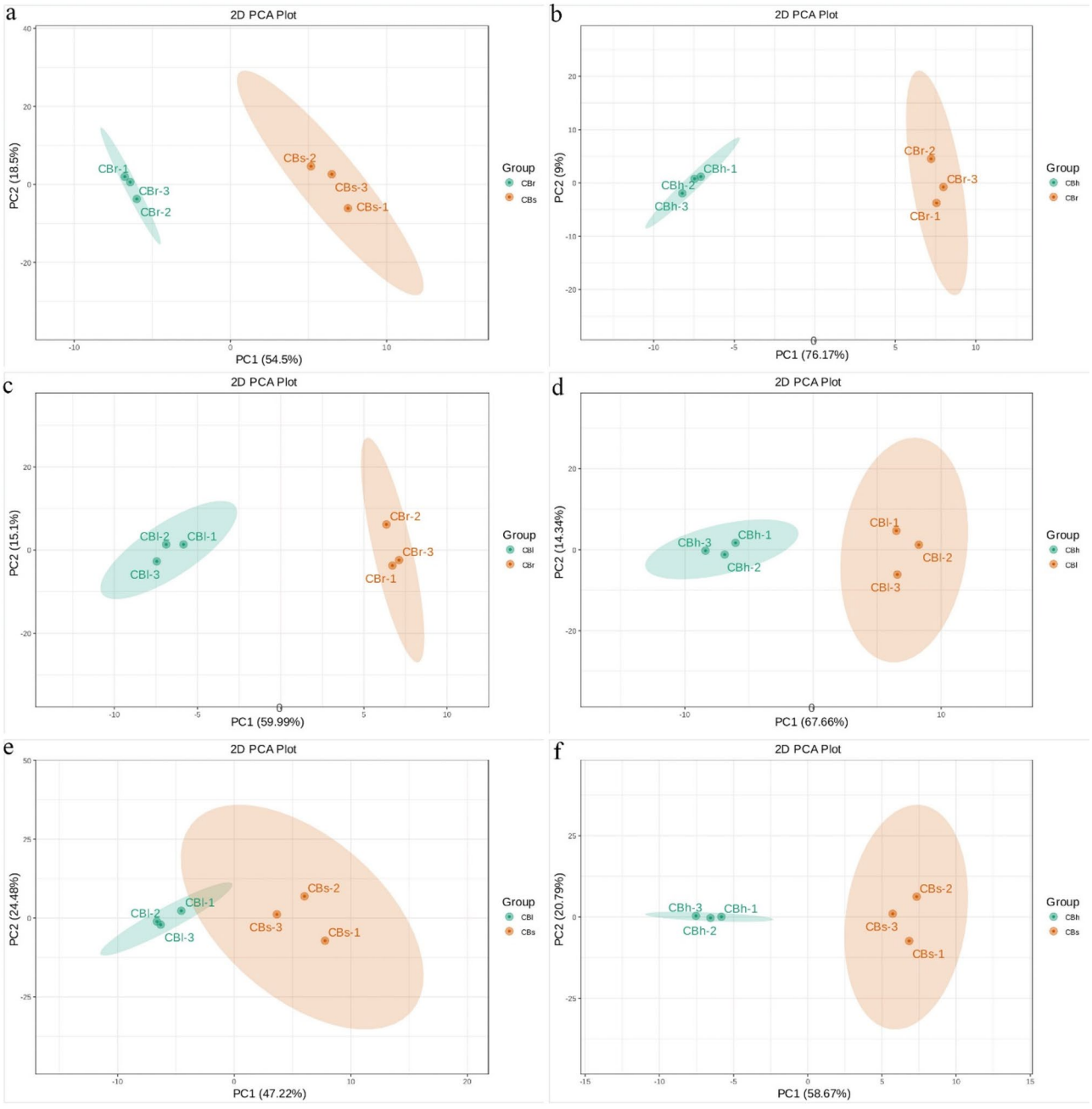

Fig. 2 OPLS-DA score plots of different tissues of *E. sonchifolia*. **a** OPLS-DA score plots in CBr and CBs comparison groups. **b** OPLS-DA score plots in CBh and CBr comparison groups. **c** OPLS-DA score plots in CBl and CBr comparison groups. **d** OPLS-DA score plots in CBh and CBl comparison groups. **e** OPLS-DA score plots in CBl and CBs comparison groups. **f** OPLS-DA score plots in CBh and CBs comparison groups

Screening of differential metabolites

A total of 69 differentially expressed metabolites (DEMs) were identified in the metabolome, categorized into 10 alkaloid classes (Supplementary Table 1). Pyrrolizidine and indole alkaloids were the most abundant, each accounting for 13% of the total (Fig. 3). To evaluate metabolic differences across *E. sonchifolia* tissues, DEMs were identified using criteria of Variable Importance in Projection (VIP) > 1 and|log2 fold-change| ≥ 1 for pairwise comparisons, there were 47 DEMs (35 down-regulated, 12 up-regulated) in the group of CBr vs. CBh, 44 DEMs (20 down-regulated, 24 up-regulated) in the group of CBl vs. CBr, 33 DEMs (17 down-regulated, 16 up-regulated) in the group of CBl vs. CBs, 48 DEMs (16 down-regulated, 32 up-regulated) in the group of CBs vs. CBr, 37 DEMs (11 down-regulated, 26 up-regulated) in the group of CBh vs. CBl, and 33 DEMs (10 down-regulated, 23 up-regulated) in the group of CBh vs. CBs.

Dynamic distribution of relative content differences in PAs

The top 10 up- and down-regulated DEMs were analyzed based on the value of the fold-change (FC), with a particular focus on PAs of which (Supplementary Tables 2 & Fig. 4a). It was found that there were 10 DEMs in the CBr vs. CBh, which were the most in each comparison group. Among them, the up-regulated metabolites (Isatidine (Isa), SnNO, Adonifoline (ADO), Erucifoline N-oxide (EfNO), Sek, Seneciphylline N-oxide (SpNO)) were more than the down-regulated metabolites (Integerrimine (INT), 3-hydroxy-1-methylpyrrolidin-2-one (HMPP), Retronecine (Re), Pyrrolidin (Py)). In the CBh vs. CBs comparison, three DEMs were identified, with up-regulated metabolites (HMPP, Re) exceeding down-regulated ones (Sek). In order to further characterize the content differences of PAs in different tissues of *E. sonchifolia*, the relative content of PAs in the four tissues of *E. sonchifolia*, including roots, stems, leaves and flowers, was compared, and the cluster heat map of relative content was drawn on the Metware cloud platform (Fig. 4b). The heat map revealed significant differences in the relative contents of Isa, SnNO, ADO, EfNO, Sek, and SpNO, with roots showing the highest levels. By contrast, HMPP, Re, and INT were most abundant in flowers, while Py peaked in leaves. It can be clearly seen from Fig. 4c that the relative content of Sek in roots far exceeded that in other tissues, and its relative content decreased in the trend of roots, stems, leaves and flowers.

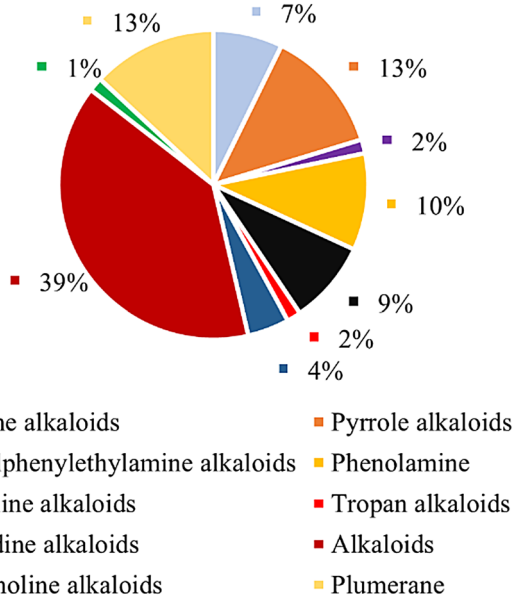

Fig. 3 The overall situation of differential metabolite alkaloids

Functional annotation and enrichment analysis of DEMs in KEGG

Kyoto Encyclopedia of Genes and Genomes (KEGG) enrichment analysis annotated 69 DEMs across 28 pathways, with significant enrichment in five key pathways (Fig. 5): ko01100 (Metabolic pathways), ko01110 (Biosynthesis of secondary metabolites), ko00999 (Biosynthesis of various plant secondary metabolites), ko00380 (Tryptophan metabolism), ko00960 (Tropane, piperidine and pyridine alkaloid biosynthesis). Among the PAs identified in DEMs, only Re and SnNO were mapped to KEGG pathway, both appearing in two shared pathways: ko01110 and ko00960.

Overall analysis of transcriptome sequencing results for *E. sonchifolia*

Transcriptome sequencing of *E. sonchifolia* tissues was conducted using the Illumina platform, yielding 80.21 Gb of Clean Data. Each sample generated over 6 Gb of Clean Data with Q30 base percentages 93% and above. Following assembly, 119,886 unigenes were identified, and subsequent analysis of transcriptome data screened 32,797 differentially expressed genes (DEGs).

Screening and analysis of DEGs

To assess gene expression differences across *E. sonchifolia* tissues, pairwise comparisons of DEGs were conducted using criteria of|log2FC| ≥ 1 and FDR < 0.05 (Fig. 6): 22,122 DEGs (10,208 down-regulated, 11,914 up-regulated) in CBr vs. CBh, 16,153 DEGs (8089 down-regulated, 8,064 up-regulated) in CBl vs. CBr, 15,650 DEGs (8507 down-regulated, 7143 up-regulated) in CBh vs. CBl, 14,706 DEGs (7583 down-regulated, 7123 up-regulated) in CBh vs. CBs, 9648 DEGs (5513 down-regulated, 4135 up-regulated) in CBs vs. CBr, 5,462 DEGs (2042 down-regulated, 3420 up-regulated) in CBl vs. CBs.

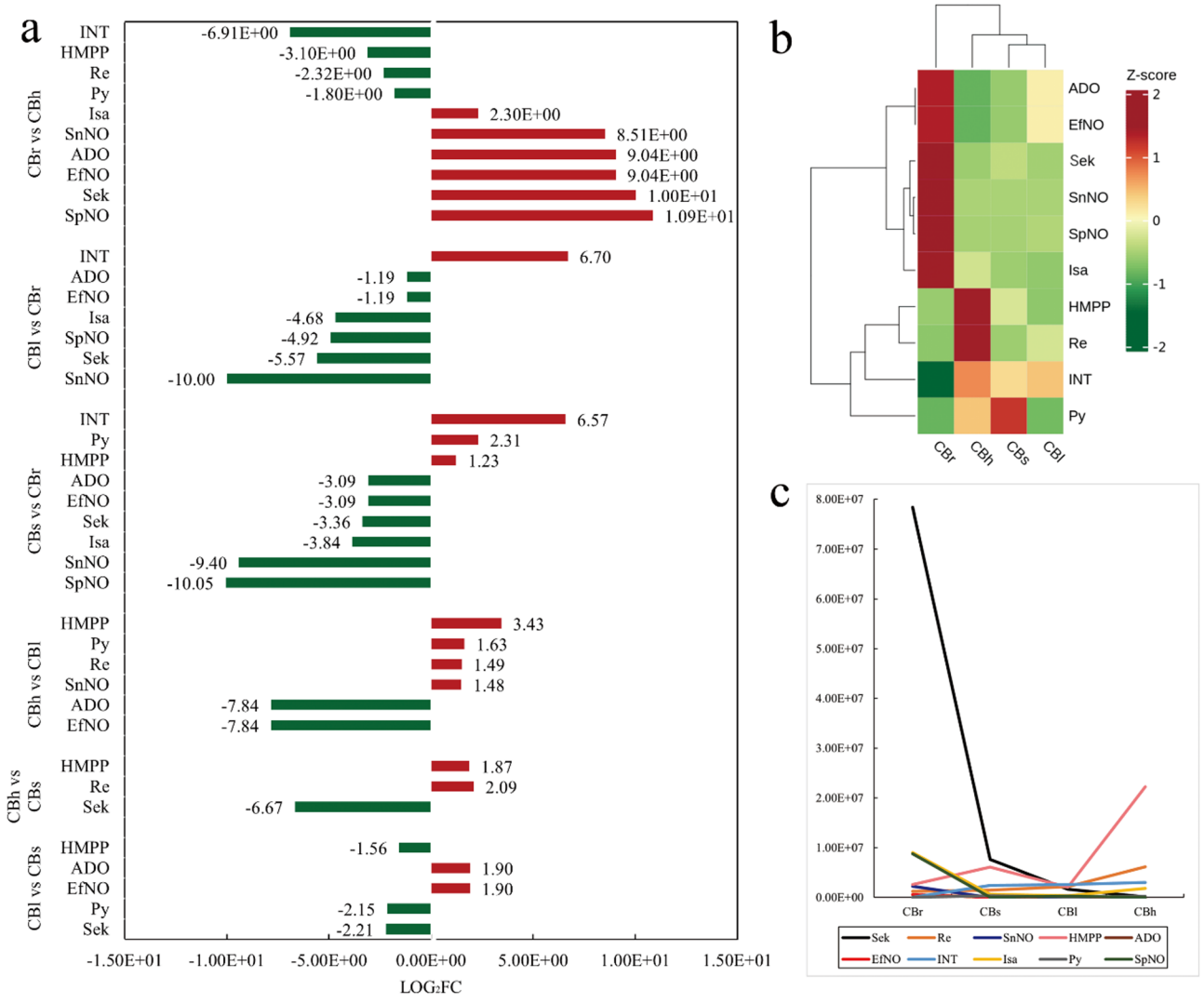

Fig. 4 Dynamic distribution of relative content difference of PAs in *E. sonchifolia*. **a** The relative content of PAs in different tissues of *E. sonchifolia*. **b** Cluster heat map of relative content of pyrrolizidine alkaloids. **c** The relative content of Sek, Re and SnNO in different tissues of *E. sonchifolia*

Functional annotation and enrichment analysis of DEGs

A total of 32,797 DEGs were annotated in 146 pathways by KEGG enrichment analysis. For each comparison group, KEGG pathways were ranked by Q-value, and the top 15 most significantly enriched pathways were combined for visualization (Fig. 7). The results showed that DEGs of *E. sonchifolia* were mainly enriched in 5 pathways: ko01100 (Metabolic pathways), ko01110 (Biosynthesis of secondary metabolites), ko04626 (Plant-pathogen interaction), ko04075 (Plant hormone signal transduction), and ko04016 (MAPK signaling pathway).

Screening of key enzyme genes of sek biosynthesis pathway in *E. sonchifolia*

Based on transcriptome data and gene expression levels (evaluated by|log2FC|), a total of 45 key enzymes (including 1 homospermidine synthase (HSS), 1 diamine oxidase, 1 cyclase, 5 alcohol dehydrogenases, 11 acyltransferases, 23 methyltransferases, 3 Pyridoxal 5′-phosphate -dependent enzymes (PLP)) were screened, spanning 7 enzyme categories (Supplementary Table 3). A total of 172 candidate key enzyme genes were identified. Using the Metware cloud platform, a gene expression heat map of these key enzymes was generated (Fig. 8), revealing significant tissue-specific expression patterns in *E. sonchifolia*. Most key enzyme genes showed markedly higher expression in roots than in flowers, followed by stems and leaves, with flowers exhibiting the lowest expression. Notably, PLP genes were highly expressed in flowers, while a subset of methyltransferase, alcohol dehydrogenase, acyltransferase, cyclase, and diamine oxidase genes showed elevated expression in stems or leaves. A heat map of the Sek biosynthetic pathway integrating key enzyme gene expression and DEMs relative contents across tissues is shown

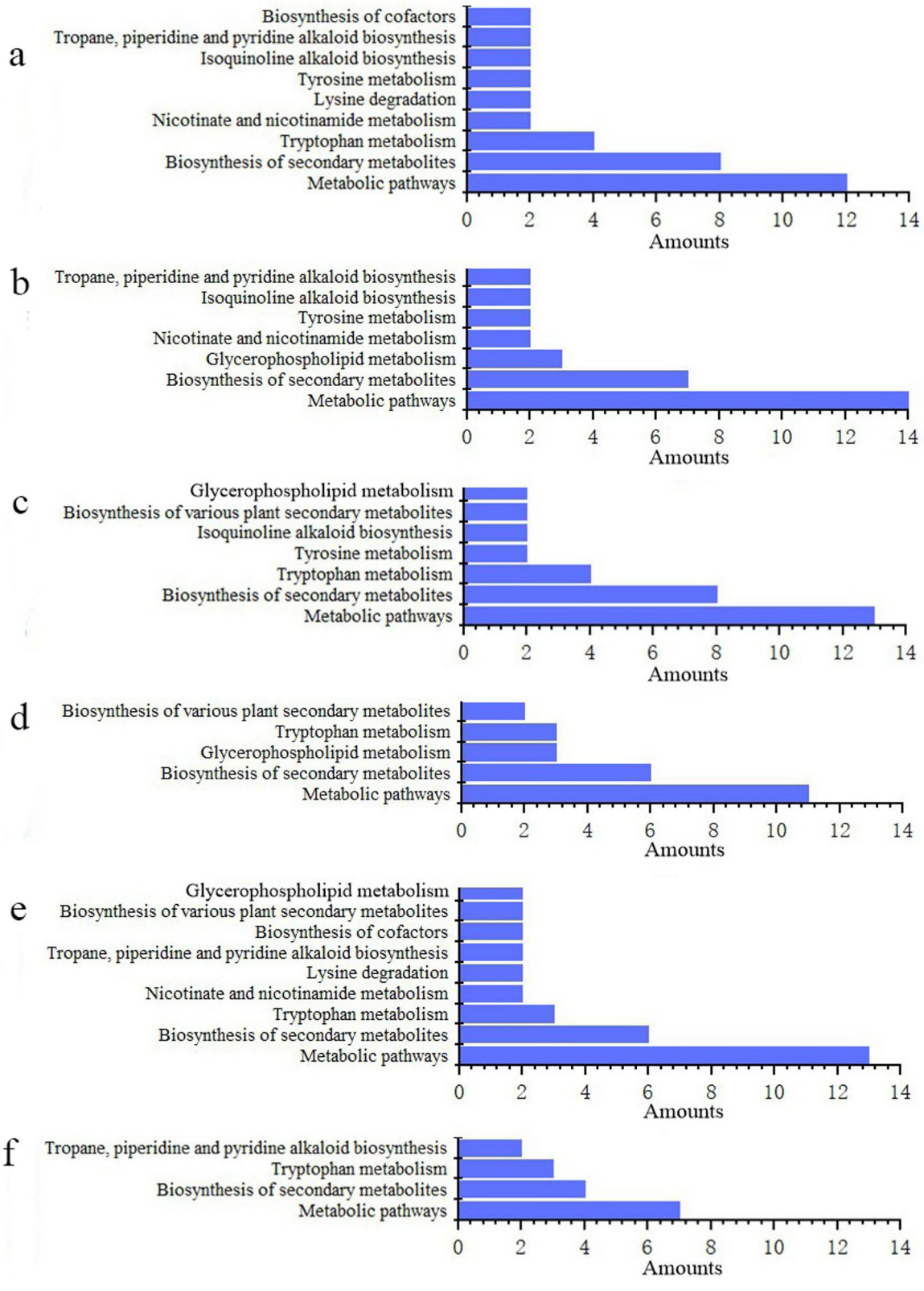

Fig. 5 The histogram of differential metabolites KEGG. **a** KEGG histogram of differential metabolites in CBr and CBh comparison groups. **b** KEGG histogram of differential metabolites in CBl and CBr comparison groups. **c** KEGG histogram of differential metabolites in CBs and CBr comparison groups. **d** KEGG histogram of differential metabolites in CBh and CBl comparison groups. **e** KEGG histogram of differential metabolites in CBh and CBs comparison groups. **f** KEGG histogram of differential metabolites in CBl and CBs comparison groups

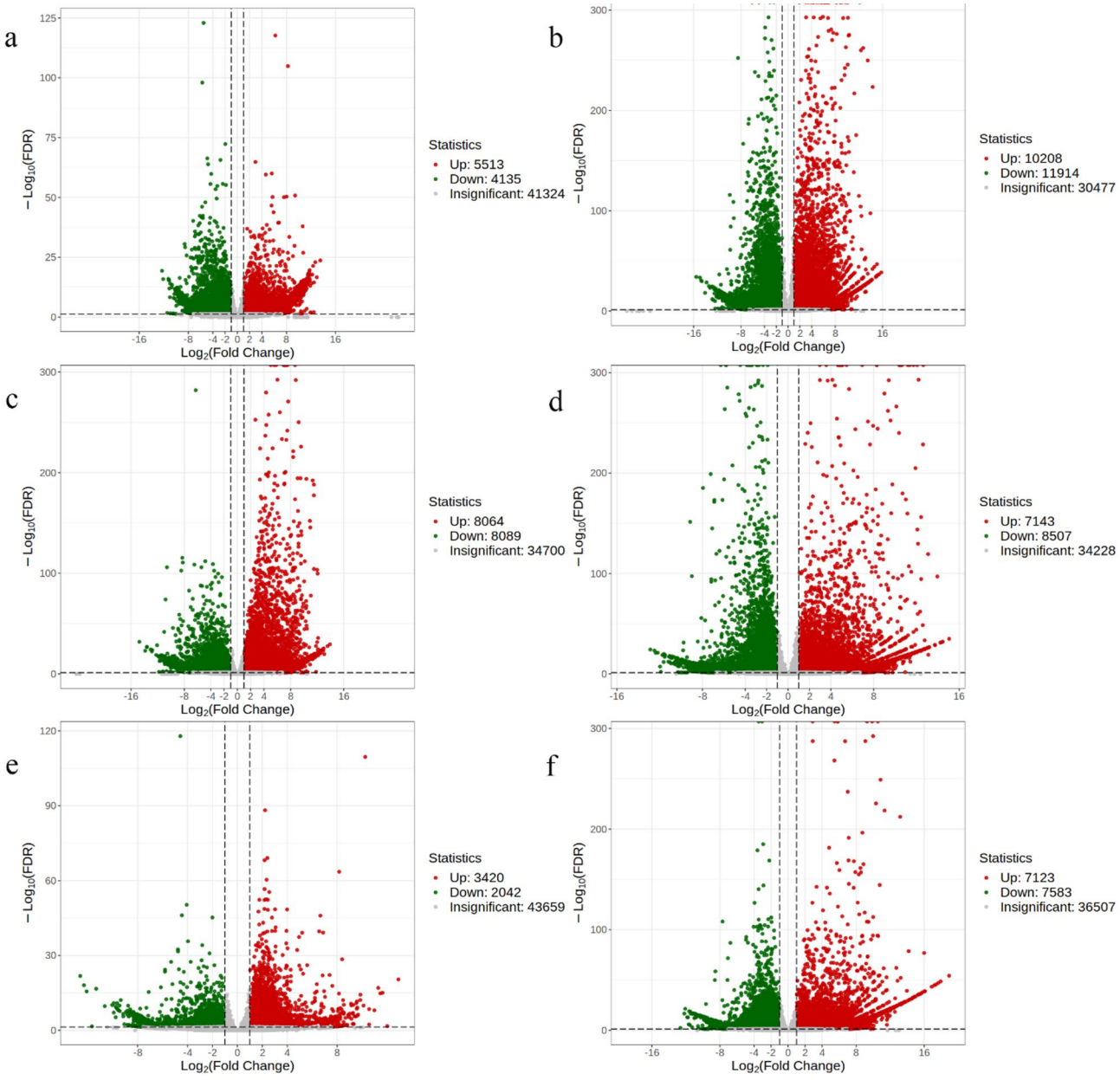

Fig. 6 Volcano map of DEGs in different tissues of *E. sonchifolia*. **a** Volcano maps of DEGs in CBr and CBs comparison groups. **b** Volcano maps of DEGs in CBh and CBr comparison groups. **c** Volcano maps of DEGs in CBl and CBr comparison groups. **d** Volcano maps of DEGs in CBh and CBl comparison groups. **e** Volcano maps of DEGs in CBl and CBs comparison groups. **f** Volcano maps of DEGs in CBh and CBs comparison groups

in Fig. 9. The results showed that HSS, diamine oxidase, cyclooxygenase, acyltransferase displayed peak expression in roots, whereas alcohol dehydrogenase (ADH) was highly expressed in both roots and stems. Most methyltransferases showed maximal expression in roots, while PLP expression was lowest in this tissue. The relative content of SnNO was highest in roots, coinciding with peak acyltransferase expression, suggesting that Re might be converted to SnNO through acyltransferase activity in roots. Additionally, Sek showed the highest relative content in roots, paralleling high methyltransferase expression and low PLP expression, implying that SnNO is likely converted to Sek through methyltransferase-mediated reactions.

Combined analysis of metabolome and transcriptomics of PAs in *E. sonchifolia*

To further explore the relationship between the relative content of PAs and the expression of key enzyme genes of the synthesis pathway of Sek in different tissues of *E. sonchifolia*, the correlation between the relative content of PAs and the expression of DEGs was compared between

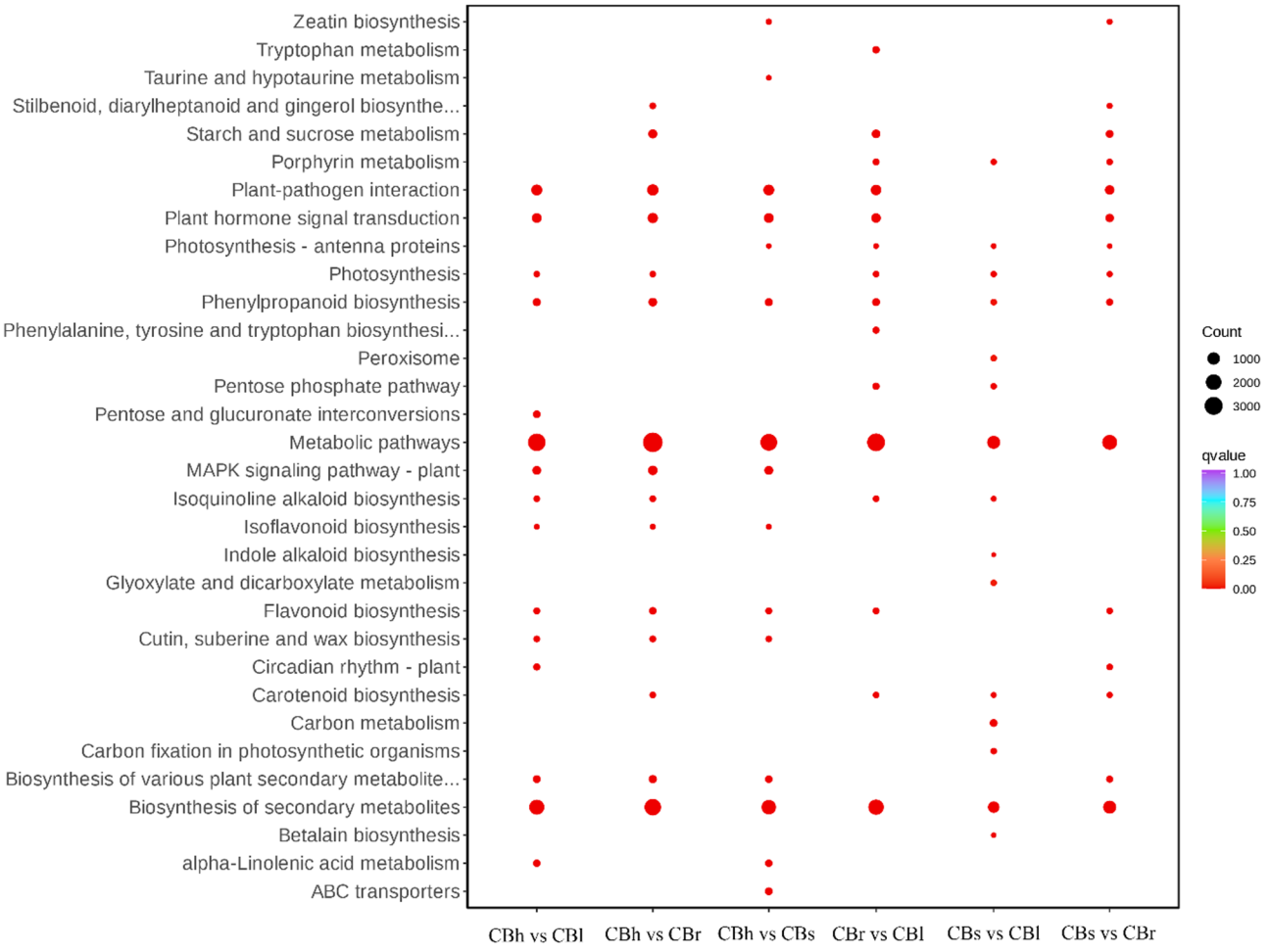

Fig. 7 Bubble map enriched by differential gene in KEGG of *E. sonchifolia*

the groups of CBr and CBh (Fig. 10). The results revealed significant correlations between differential metabolites and DEGs. Specifically, Sek, SnNO, SpNO, Isa, ADO, and EfNO showed significant positive correlations with DEGs, whereas INT exhibited a significant negative correlation. These correlations were observed for DEGs encoding enzymes K1, K2, K3, K4 and K5.

Screening of transcription factors related to the biosynthesis of sek in *E. sonchifolia*

The co-expression network of genes and transcription factors (TFs) was constructed according to the co-expression relationship between genes related to the biosynthesis of Sek and TFs (Fig. 11). The analysis identified three TFs of ERF-ERF, AP2, and SET putatively associated with Sek biosynthesis. Co-expression network results showed that the SET TF was closely linked to genes Cluster-65449.2 ([histone H3]-lysine4 N-trimethyltransferase MLL3), Cluster-64513.1 ([histone H3]-lysine4 *N*-trimethyltransferase MLL3) and Cluster-59406.3 ([histone H3]-lysine4 *N*-trimethyltransferase MLL3). Additionally, AP2 and SET TFs were significantly co-expressed with the gene of Cluster-61885.4 (glycine hydroxymethyltransferase).

qRT-PCR expression analysis of key enzyme genes

The 5 candidate gene sequences with the largest multiplicity of difference (CBr vs CBh) among the key enzymes of the Sek biosynthetic pathway of *E. sonchifolia* were selected for qRT-PCR validation. Using flowers as the control, the relative expression of four candidate genes, *BAHD-Ats* (BAHD acyltransferase gene), *CCoAOMT* (caffeoyl-CoA O-methyltransferase gene), *BOMT* (benzoate *O*-methyltransferase gene) and *3AT* (anthocyanidin 3-*O*-glucoside 6”-*O*-acyltransferase gene), was highest in roots, while the relative expression level of *CAD* (cinnamyl-alcohol dehydrogenase gene) exhibited peak expression in stems. The relative expression of *BOMT* was roots, stems, leaves and flowers in turn. The relative expression levels of *BAHD-Ats* and *3AT* were roots, stems, flowers and leaves in turn, while *CAD* expression followed stems, flowers, roots and leaves in turn. In

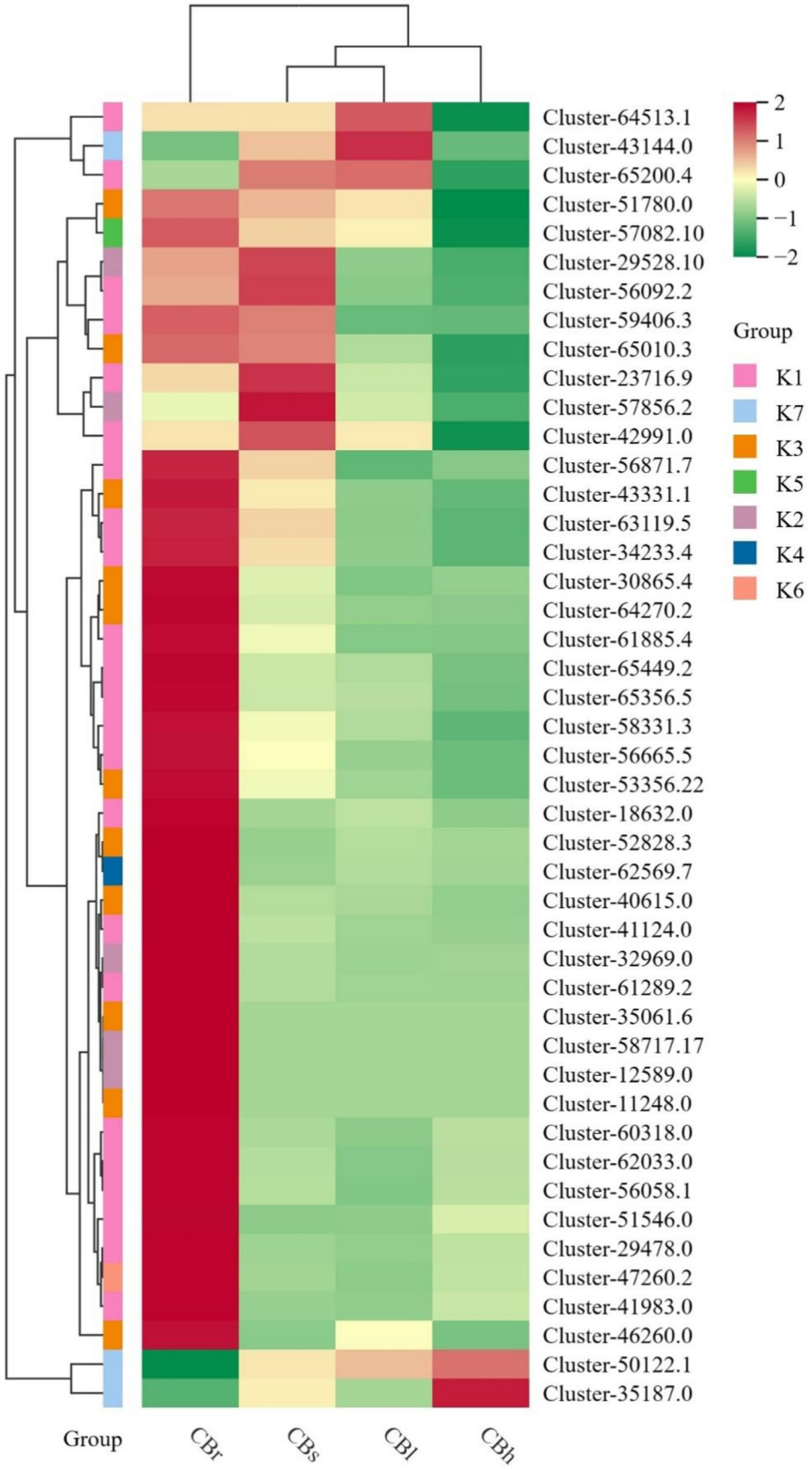

Fig. 8 Differential gene expression quantity heat map of *E. sonchifolia*

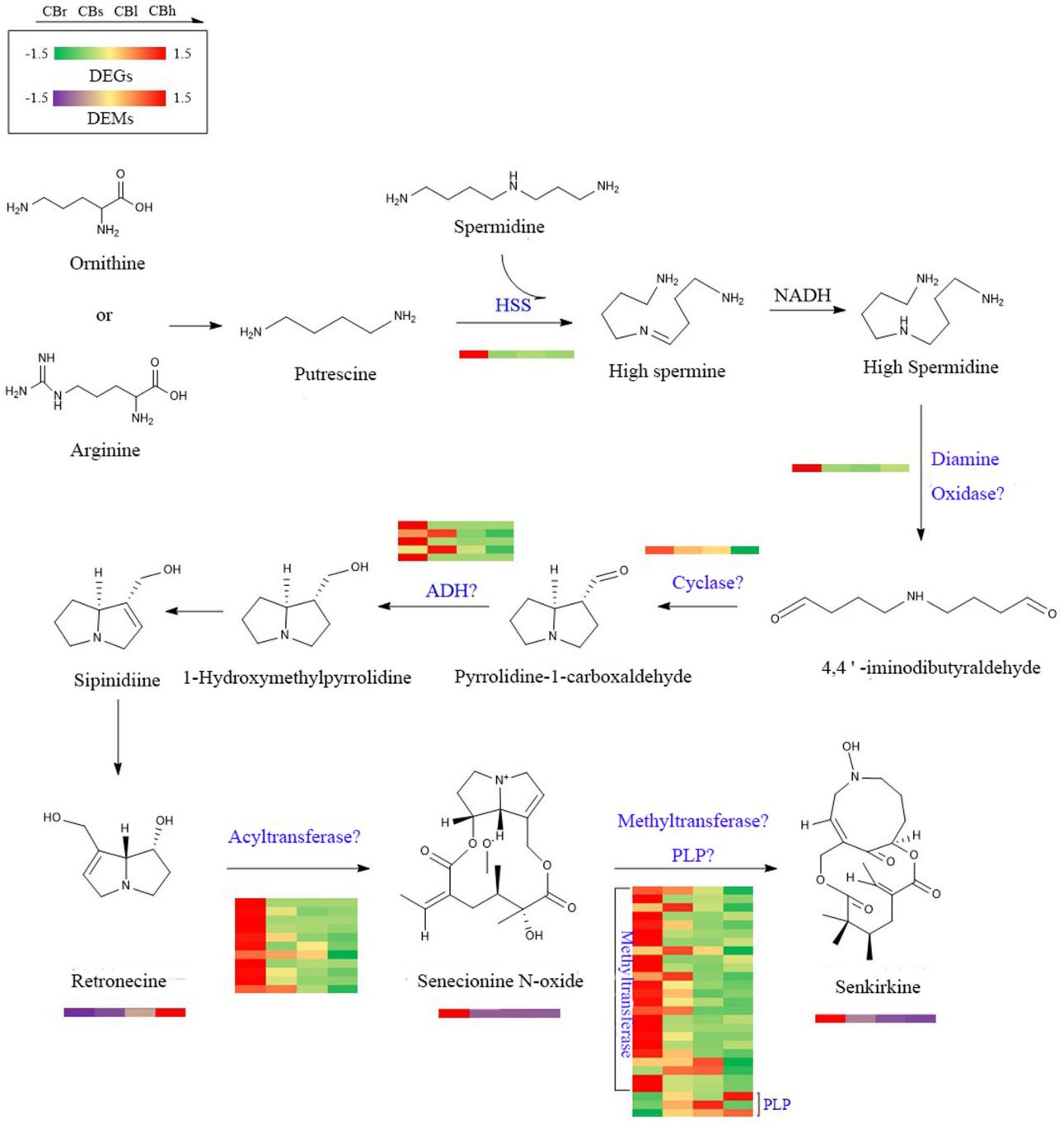

Fig. 9 Pathway heat map of Sek biosynthetic pathway in *E. sonchifolia*

contrast to roots, *CCoAOMT* expression was negligible in stems, leaves and flowers (Fig. 12).

Discussion

There are limited reports on the research of PAs in *E. sonchifolia*, and no comprehensive analysis has been conducted on PAs in this plant. In this study, metabolomics and transcriptome sequencing detected a total of 91 DEMs, categorized into 10 types of alkaloids, and screened 32,797 DEGs. Among the DEMs, up-regulated metabolites outnumbered down-regulated ones, while down-regulated genes exceeded up-regulated genes among the DEGs. Notably, the relative contents of PAs varied significantly across different tissues of *E. sonchifolia*, with Sek exhibiting the highest content in roots and the lowest in flowers. Sek and SnNO were significantly up-regulated metabolites, whereas Re was a significantly down-regulated metabolite.

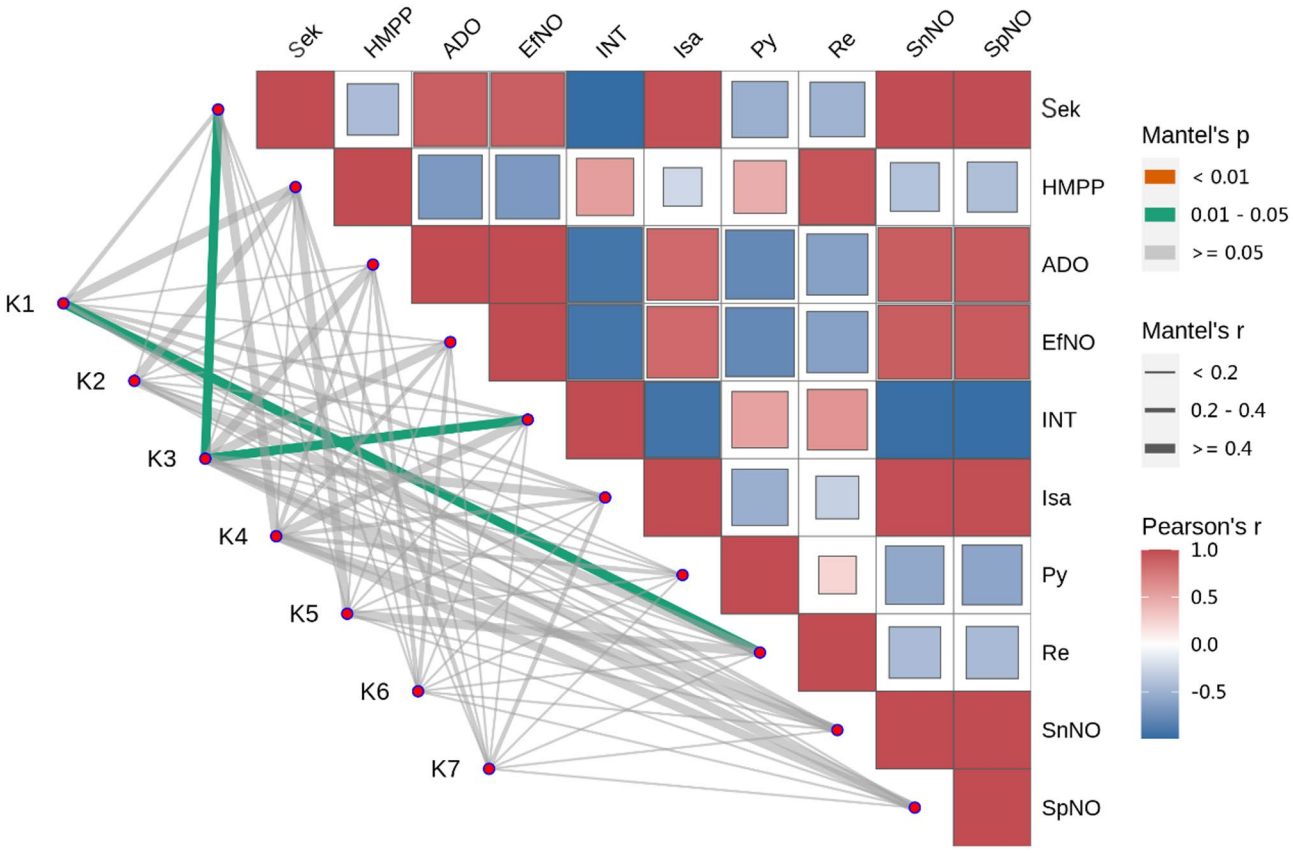

Fig. 10 Correlation analysis between differential metabolites and DEGs in CBr and CBh groups. "K1" is methyltransferase, "K2" is alcohol dehydrogenase [32], "K3" is acyltransferase [33], "K4" is HSS [33], "K5" is cyclase, "K6" is diamine oxidase [34], "K7" is 5'-pyridoxal phosphate-dependent bifunctional enzyme (PLP) [35].

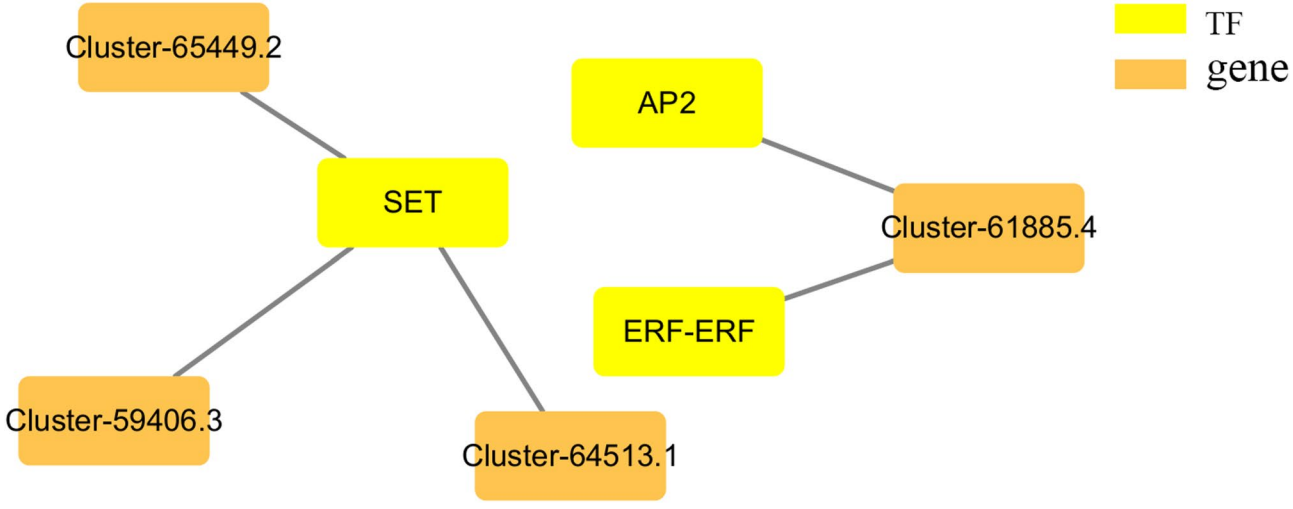

Fig. 11 Co-expression network of genes and transcriptional factors involved in flavonoid Sek biosynthesis

Studies have shown that PAs form spermine by ornithine or arginine under the action of decarboxylase, followed by hydrolysis to form putrescine [36]. Putrescine reacts with spermidine under the action of HSS to generate homospermidine, followed by NADH-dependent reduction to high spermidine, and cyclization to form a pyrrole dialkyl skeleton [33], Subsequent modifications, including oxidation, reduction, acylation, and methylation, yield alkaloids such as Re, SnNO, and Sek [32]. The PAs synthetic pathway is relatively complex, currently,

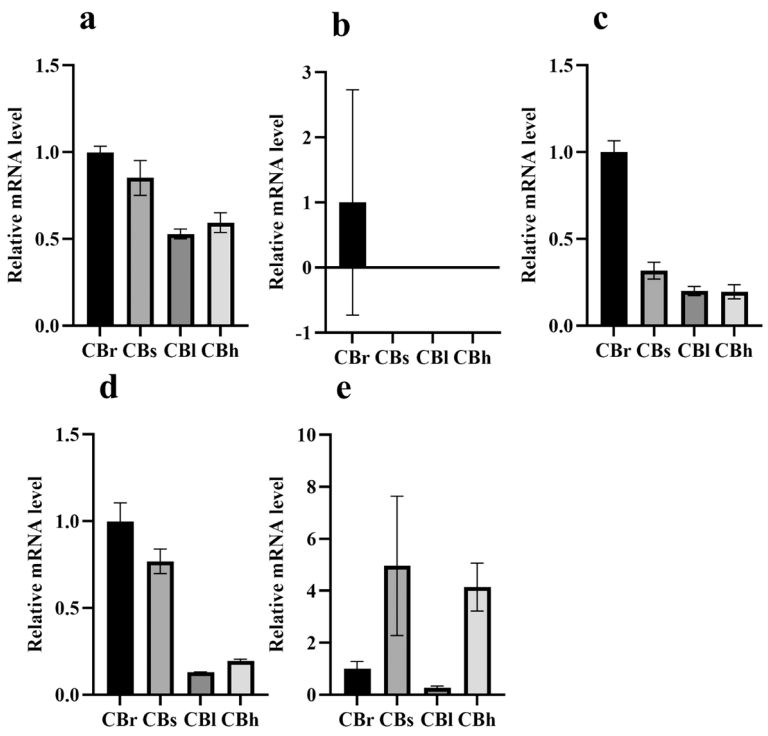

Fig. 12 Relative expression of target genes. **a** Relative expression of gene "*BAHD-Ats*". **b** Relative expression of gene "*CCoAOMT*". **c** Relative expression of gene "*BOMT*". **d** Relative expression of gene "*3AT*" **e** Relative expression of gene "*CAD*". "*BAHD-Ats*" is a BAHD acyltransferase gene, "*CCoAOMT*" is a caffeoyl-CoA *O*-methyltransferase gene, "*BOMT*" is a benzoate *O*-methyltransferase gene, "*3AT*" is an anthocyanidin 3-*O*-glucoside 6"-*O*-acyltransferase gene, and "*CAD*" is a cinnamyl-alcohol dehydrogenase gene

only HSS has been characterized, and other key enzymes that have not yet been characterized are yet to be explored. To further analyze the Sek synthesis pathway, we screened 45 key enzymes from the biosynthetic pathway based on transcriptome data, belonging to 7 categories with 172 candidate enzyme genes. The expression of these key enzyme genes differed significantly among tissues, with roots showing notably higher expression than flowers. Integrated analysis of metabolome and transcriptome data revealed a significant correlation between differential metabolites and DEGs, including methyltransferase, alcohol dehydrogenase, acyltransferase, HSS, and cyclase genes.

At present, there is no report on the regulation of enzyme reaction in Sek biosynthesis pathway by related TFs. This study identified potential TFs involved in regulating Sek biosynthesis, such as those from the SET, AP2, and ERF-ERF families. Among them, the TF of SET was co-expressed with the gene of Cluster-65449.2 ([histone H3]-lysine4 N-trimethyltransferase MLL3), Cluster-64513.1 ([histone H3]-lysine4 N-trimethyltransferase MLL3) and Cluster-59406.3 ([histone H3]-lysine4 N-trimethyltransferase MLL3), and the TFs of AP2 and ERF-ERF were co-expressed with the gene of Cluster-61885.4 (glycine hydroxymethyltransferase). The results showed that the TFs of ERF-ERF, AP2 and SET may regulate the transcription of glycine hydroxymethyltransferase and [histone H3]-lysine4 *N*-trimethyltransferase MLL3, and further regulate the methylation process of the synthesis pathway of Sek. The AP2 and ERF transcription factor families are of great significance in plant growth and development, the response to various stresses, hormone signal transduction, and metabolic regulation [37, 38]. Notably, while this study identified potential TF-gene interactions that may regulate Sek biosynthesis, experimental validation of these regulatory relationships remains pending. Additionally, the specific roles of key enzymes in the Sek synthetic pathway require further functional elucidation through molecular biology techniques. Future studies will focus on experimentally verifying the regulatory mechanisms of these TFs and elucidating the roles of candidate enzymes in PAs biosynthesis.

By using qRT-PCR with ubiquitin-protein ligase (*UPL*) gene as a stable internal reference gene, we verified that when flowers served as the control group, four key enzyme genes (*BAHD-Ats*, *CCoAOMT*, *BOMT*, and *3AT*) all showed the highest relative expression in roots. In contrast, *CAD* exhibited the highest relative expression in stems, which was basically in line with the pattern of transcriptome data. These results suggest distinct expression patterns of key enzymes in the Sek biosynthetic

pathway, implying that roots tissues may serve as the primary site for Sek accumulation. Additionally, the differential expression of *CAD* in stems further indicates potential tissue-specific regulatory mechanisms for PAs biosynthesis, possibly associated with secondary metabolism in vascular tissues. Such findings have laid a solid foundation for exploring the spatial regulation of alkaloid biosynthesis in *E. sonchifolia*.

Conclusion

In this study, integrative metabolomic and transcriptomic analyses identified 45 key enzymes in the Sek biosynthesis pathway, spanning 7 functional categories and encompassing 172 candidate enzyme genes. qRT-PCR validation was performed on the top 5 candidate gene sequences with the highest fold changes. The results showed that four key enzyme genes (*BAHD-Ats*, *CCoAOMT*, *BOMT*, *3AT*) exhibited peak expression in roots, while *CAD* showed maximal expression in stems, findings consistent with transcriptome data. These results provided a reference for the functional expression analysis of *E. sonchifolia*, and laid a foundation for the future analysis of synthesis pathway of Sek and the regulation of key enzyme genes of toxic components, so as to obtain low-toxic raw materials of *E. sonchifolia*.

Materials and methods

Plant material collection

The sample of *E. sonchifolia* (L.) DC. was collected on August 17, 2023 in Qingxiu District, Nanning City, Guangxi Zhuang Autonomous Region, preserved in Guangxi University of Chinese Medicine Herbarium, numbered 20235090002. It was identified as the whole grass of *E. sonchifolia* (L.) DC. by professor Wang Liuping of Guangxi University of Chinese Medicine.

After collecting the whole plant of *E. sonchifolia*, wash, dry, divide the roots, stems, leaves and flowers, put them into 15 ml centrifuge tubes, number them, put them into liquid nitrogen for quick freezing, and store them in an ultra-low temperature refrigerator at − 80 ℃ for spare tissues.

Metabolome sequencing of *E. sonchifolia*

The 4 samples of roots, stems, leaves and flowers of *E. sonchifolia* were taken from the ultra-low temperature refrigerator, each with 3 biological replicates, and divided into two tissues. One was sent to Wuhan Metware Biotechnology Inc for the analysis of UPLC-MS/MS. The conditions of UPLC analysis were as follows: column: Agilent SB-C18 (1.8 μm, 2.1 mm × 100 mm); mobile phase A (ultrapure water) with 0.1% formic acid, and mobile phase B (acetonitrile) with 0.1% formic acid; gradient elution: 0–9 min, 5%–95% B; 9–10 min, 95% B; 10–11.1 min, 95% B; and 10–11.1 min.; 10–11.1 min, 5% B; 11.1–14 min, 5% B; flow rate 0.35 mL/min; column temperature 40 ℃; injection volume of 2 μl. Mass spectrometry (MS) conditions: ESI temperature 550 ℃, mass spectrometry voltage 5500 V (positive ion mode), mass spectrometry voltage − 4500 V (negative ion mode), ion source gas I (GSI), gas II (GSII), and curtain gas (CUR) were set to 50, 60, and 25 psi, respectively. The chromatographic peaks of the target metabolites were scanned and detected using the MRM mode of a triple quadruple pole, and the TIC plots of the mass spectrometry detection analyses of the different QC samples were analyzed by overlapping display. The metabolome data obtained from UPLC-MS/MS detection and analysis were analyzed, and the PCA was performed on all the samples to observe the inter- and intra-group differences of different tissues of *E. sonchifolia*, based on the OPLS-DA, the VIP and FC values obtained from univariate analysis were used to further analyze and screen for DEMs. DEMs were further analyzed and screened by setting VIP > 1 and|log2FC| ≥ 1 as the thresholds for DEMs, and the KEGG database was used for KEGG annotation and enrichment analysis of the screened DEMs.

Transcriptome sequencing of *E. sonchifolia*

Another copy of the same samples used for transcriptome sequencing, a total of 12 samples, were sent to Wuhan Metware Biotechnology Inc for transcriptome sequencing analysis using the Illumina platform.

RNA quantification and qualification

RNA degradation and contamination was monitored on 1% agarose gels. RNA purity was checked using the NanoPhotometer® spectrophotometer (IMPLEN, CA, USA). RNA concentration was measured using Qubit® RNA Assay Kit in Qubit®2.0 Flurometer (Life Technologies, CA, USA). RNA integrity was assessed using the RNA Nano 6000 Assay Kit of the Bioanalyzer 2100 system (Agilent Technologies, CA, USA).

Library preparation for transcriptome sequencing

A total amount of 1 μg RNA per sample was used as input material for the RNA sample preparations. Sequencing libraries were generated using NEBNext® UltraTM RNALibrary Prep Kit for Illumina® (NEB, USA) following manufacturer's recommendations and index codes were added to attribute sequences to each sample. Briefly, mRNA was purified from total RNA using poly-T oligoattached magnetic beads. Fragmentation was carried out using divalent cations under elevated temperature in NEBNext First Strand Synthesis Reaction Buffer (5X). First strand cDNA was synthesized using random hexamer primer and M-MuLVReverse Transcriptase (RNase H-). Second strand cDNA synthesis was subsequently performed using DNA Polymerase I and RNase H.

Remaining overhangs were converted into blunt ends via exonuclease/polymerase activities. After adenylation of 3' ends of DNA fragments, NEBNext Adaptor with hairpin loop structure were ligated to prepare forhybridization. In order to select cDNA fragments of preferentially 250–300 bp in length, the library fragments were purified with AMPure XP system (Beckman Coulter, Beverly, USA). Then 3 μl USER Enzyme (NEB, USA) was used with size-selected, adaptor-ligated cDNA at 37 °C for 15 min followed by 5 min at 95 °C before PCR. Then PCR was performed with Phusion High-Fidelity DNA polymerase, Universal PCR primers and Index (X) Primer. Atlast, PCR products were purified (AMPure XP system) and library quality wasassessed on the Agilent Bioanalyzer 2100 system.

Clustering and sequencing

The clustering of the index-coded samples was performed on a cBot Cluster Generation System using TruSeq PE Cluster Kit v3-cBot-HS (Illumia) according to the manufacturer's instructions. After cluster generation, the library preparations were sequenced on an Illumina platform and 150 bp paired-end reads were generated.

Data QC

Use fastp to filter the original data, mainly to remove reads with adapters; when the N content in any sequencing reads exceeds 10% of the base number of the reads, remove the paired reads; when any sequencing reads When the number of low-quality ($Q <= 20$) bases contained in reads exceeds 50% of the bases of the reads, these paired reads will be removed. All subsequent analyses are based on clean reads.

Transcriptome assembly

Transcriptome assembly was performed using Trinity. Corset was used to regroup relevant transcripts into 'gene' clusters (https://github.com/trinityrnaseq/trinityrnaseq).

CDS prediction

Use TransDecoder (https://github.com/TransDecoder/TransDecoder/wiki) to identify candidate coding regions within transcript sequences generated by de novo RNA-Seq transcript assembly using Trinity.

Gene functional annotation

KEGG functional annotation and enrichment analysis of the DEGs were performed using the database of KEGG.

Quantification of gene expression levels

Gene expression levels were estimated by RSEM, and then calculate the FPKM of each gene based on the gene length. FPKM is currently the most commonly used method to estimate gene expression levels.

Differential expression analysis

Differential expression analysis between the samples was performed using DESeq2. The P value was corrected using the Benjamini & Hochberg method. The corrected P value and|log2FC| are used as the threshold for significant difference expression.

Transcription factor analysis

TF analysis was performed using iTAK, which integrates two databases, PlnTFDB and PlantTFDB.

The qRT-PCR verification of key enzyme genes

The first 5 candidate gene sequences with the largest|log2FC| in the key enzymes for Sek synthesis in the CBr vs. CBh group were selected. The *UPL* gene was used as the internal reference gene, and the specific primers were designed using Premier 5.0 (Supplementary Table 4). The primers were synthesized by Nanning Jenice Biotechnology Co., Ltd. The total RNA was extracted from different tissues of *E. sonchifolia* using the Eastep®Super Total RNA Extraction Kit, and its concentration and quality were detected and then reverse transcription reaction into cDNA was performed according to the instructions of the reverse transcription kit. The first incubation system was 16 μl, the second incubation system was 20 μl, and 3 technical replicates were set for each sample. The transcribed cDNA was diluted 350-fold with RNase-Free ddH_2O and used as the gene template. The reaction system was configured according to the instructions of the ChamQ SYBR qPCR Master Mix kit, and the reaction was performed according to 95 ℃ 3 min, 95 ℃ 10 s, 60 ℃ 30 s, 95 ℃ 10 s, 65 ℃ 6 s, 95 ℃ 50 s, 39 cycles of the amplification procedure were validated by qRT-PCR, and the relative expression of the candidate genes was calculated using the formula of $2^{-\Delta\Delta Ct}$, in which each sample was repeated 3 times. The specific expression patterns of the screened synthesis key enzyme candidate genes of the synthesis of Sek in different tissues of *E. sonchifolia* were researched and jointly analyzed with transcriptomic data and metabolomic data to preliminarily validate the function of the biosynthesis key enzyme gene of Sek in *E. sonchifolia*.

Acknowledgements

Not applicable.

Author contributions

Y: Methodology, Software, Writing - original draft. Q: Resources, Methodology, Software. T: Supervision, Conceptualization, Methodology, Writing - review & editing. H: Resources, Conceptualization. L: Conceptualization, Resources. C: Resources, Methodology. M: Resources, Conceptualization. Z: Resources, Methodology. X: Resources, Methodology.All authors reviewed the manuscript.

Funding
This work was supported by the Guangxi Natural Science Foundation Project (2022JJA140897), Inheritance and innovation team of Guangxi Traditional Chinese Medicine (2022B005), Guangxi University of Traditional Chinese Medicine Guipai Xinglin Young Talents (2022C033), and the Guangxi Zhuang Autonomous Region University Huang Danian style teacher team "Chinese medicine inheritance innovation teacher team" (Gui Jiao teacher [2023] No. 31).

Data availability
The sequence data supporting the results of this study have been stored in the NCBI database. The main accession number is PRJNA1189669, and the website is https://www.ncbi.nlm.nih.gov/bioproject/?term=PRJNA1189669.

Declarations

Ethics approval and consent to participate
The methods involved in this study were carried out in compliance with local and national regulations.

Consent for publication
Not applicable.

Competing interests
The authors declare no competing interests.

Received: 11 November 2024 / Accepted: 16 July 2025
Published online: 01 August 2025

References

1. Ning Y, Zhu C, Mo J, et al. Determination of sek in herba Emiliae by HPLC. Drug Stand China. 2014;15:269–72.
2. Zou X, Zhao C, Gong X, et al. Chemical constitutes *Emilia Sonchifolia (L.) DC*. Chin Pharm J. 2012;47:1891–4.
3. Lan L, Du Y, He T, et al. Research progress on *Emilia sonchifolia (L.) DC.* of traditional Chinese medicine. Yunnan J Tradit Chin Med Materia Med. 2009;30:61.
4. Hou E, Liu B, Ni S, et al. Overview of pharmaceutical research on *Emilia Sonchifolia (L.) DC*. Northwest Pharm J. 2009;24:432–3.
5. Liang L, Chen S, Lu W, et al. Research progress on chemical constituents, Pharmacological effects and clinical application of Zhuang medicine Yidianhong. J Med Pharm Chin Minorities. 2021;27:75–8.
6. Couto M, Vilela C, Dias F, et al. Antinociceptive effect of extract of *Emilia Sonchifolia* in mice. J Ethnopharmacol. 2011;134:348–53.
7. The Pharmacopoeia Committee. Pharmacopoeia of the people's Republic of China. Beijing: China Pharmaceutical Science and Technology; 2015.
8. Zhao D, Sun X, Zhou X, et al. Research progress on chemical constituents and Pharmacological effects of Emilia plants. Chin Traditional Patent Med. 2019;41:1654–61.
9. Yang H, Wei M, Cui D. The resource value and market prospect of a little red of Asteraceae plants. Chin Wild Plant Resour. 2009;28:44–5.
10. Wang L, Chen L, Zhang Y, et al. Isolation of chemical constituents of *Emilia Sonchifolia* and determination of Protocatechuic acid. J Guangxi Univ (Natural Sci Edition). 2014;39:1366–70.
11. Wang W. Study on the extraction and antioxidant and anti-inflammatory activities of total flavonoids from monosaccharide. College of Chemistry and Chemical Engineering, Guangxi University. 2011.
12. Chen L. Separation, analysis of chemical constituents and study on antioxidant activity of *Emilia Sonchifolia*. Guangxi University. 2015.
13. Ni X. Extraction, separation and bioactivity of *Emilia Sonchifolia* polysaccharide and alkaloids. Guangxi University. 2013.
14. Cheng D, Röder E. Pyrrolizidine alkaloids from *Emilia Sonchifolia*. Planta Med. 1986;484–6.
15. Shen S. Study on chemical constituents and quality control of *Emilia Sonchifolia*. Peking Union Medical College. 2013.
16. Zhou W, Li J, Wei Y, et al. Determination of total alkaloids in *Emilia Sonchifolia* collected at different harvesting time in Guangxi. Food Sci. 2009;30:151–4.
17. Hsieh C, Chen H, Lee C, et al. Hepatotoxic pyrrolizidine alkaloids in *Emilia Sonchifolia* from Taiwan. Food Wkly Focus. 2015;42:1–7.
18. Luo Z, Li X, Lu W, et al. Development of UPLC-Q-TOF-MS coupled with cation-exchange solid-phase extraction method for the determination of ten pyrrolizidine alkaloids in herbal medicines. Anal Sci. 2019;35:1317–25.
19. Shen S, Zhang Y, Shen L, et al. Progress on chemical constituents and pharmacological activities of genus emilia. Chin J Exp Tradit Med Formulae. 2012;18:308.
20. Liang A, Ye Z. General situation of the toxicity researches on senecio. China J Chin Materia Med 2006;93–7.
21. Tang j, Hattori M. Pyrrolizidine alkaloids-containing Chinese medicines in the Chinese pharmacopoeia and related safety concerns. Acta Pharm Sinica. 2011;46:762–72.
22. Gao J, Wang C, Li Y, et al. Advance on Pharmacologic actions, toxicity and pharmacokinetics of pyrrolizidine alkaloids. China J Chin Materia Med. 2009;34:506–11.
23. Wang T, Song H. Research progress and risk analysis on hepatotoxicity of pyrrolizidine alkaloids. Herald Med. 2018;37:1033–77.
24. Guo Y, Zhang S, Wen L, et al. Clinical features of sinusoidal obstruction syndrome induced by pyrrolidine alkaloids in China. J Clin Hepatol. 2018;34:1277–81.
25. Chen R, Zhuo H, Li X, et al. Hepatic sinusoidal obstruction syndrome induced by Chinese herb *Emilia Sonchifolia* (L.) DC: A case report. J Clin Hepatol. 2019;35:2778–9.
26. Zhang Y, Ma S, Yang F, et al. Status of content analysis of pyrrolizidine alkaloids in food and herbs. China J Chin Materia Med. 2020;45:5421–8.
27. Zan K, Zhou Y, Li Y, et al. Simultaneous determination of six pyrrolizidine alkaloids in different tissues of *Emilia Sonchifolia* by UPLC-MS/MS. China J Chin Materia Med. 2021;46:4456–61.
28. Qiao Y. Analysis and detection of pyrrolizidine alkaloids and nitrogen oxides in Chinese pharmacopoeia. Peking Union Medical College. 2020.
29. You L, Song H, Luo M et al. Gene knockout of effector protein G12593 of banana Fusarium wilt fungus. In: Proceedings of the 2023 Annual Conference of the Chinese Society of Plant Pathology. Zhongkai Agricultural Engineering Institute Plant Health Innovation Institute, Guangzhou. 2023.
30. Xu M, Xu J, Guo M, et al. Functional analysis of the chitin deacetylase family in the pathogenesis of Fusarium graminis. In: Proceedings of the 2023 Annual Conference of the Chinese Society of Plant Pathology. College of Plant Protection, State Key Laboratory of Crop Stress Biology in Arid Regions, Northwest A&F University, Xianyang. 2023.
31. Zhang Y, Liu N, Li B, et al. Study on the function of BdGpmk1-MAPK signaling pathway in Apple fungus. In: Proceedings of the 2023 Annual Conference of the Chinese Society of Plant Pathology. College of Plant Medicine, Qingdao Agricultural University, Shandong Provincial Key Laboratory of Plant Pest Control and State Key Laboratory of Plant Pest Biology, Qingdao. 2023.
32. Han H, Jiang C, Wang C, et al. Pyrrolizidine alkaloids in tea: A review of analytical methods, contamination levels and health risk. Food Sci. 2021;42:255–66.
33. Ober D, Hartmann T. Homospermidine synthase, the first pathway-specific enzyme of pyrrolizidine alkaloid biosynthesis, evolved from Deoxyhypusine synthase. Proc Natl Acad Sci USA. 1999;96:14777–82.
34. Zhang Y, Lu Y, Shi B, et al. Research progress on metabolism and physiological function of polyamines in plants. North Hortic. 2023;15:122–7.
35. Dai G, Han W, Mei Y, et al. Pyridoxal-5'-phosphate-dependent bifunctional enzyme catalyzed biosynthesis of indolizidine alkaloids in fungi. Proc Natl Acad Sci USA. 2020;117:1174–80.
36. Li S, Duan Y, Huang Y. Discovery and biosynthesis of bacterial pyrrolizidine alkaloids. Microbiol China. 2021;48:2437–53.
37. Feng K, Hou X, Xing G, et al. Advances in AP2/ERF super-family transcription factors in plant. Crit Rev Biotechnol. 2020;40:750–76.
38. Chen G, Shao T, Zhou Y, et al. Analysis of the Aging-Related AP2/ERF transcription factor gene family in osmanthus Fragrans. Int J Mol Sci. 2024;25:8025–8025.

Publisher's note